

# Bulk Magnetic Properties and Phase Diagram of Li-doped $\text{La}_2\text{CuO}_4$ : Comparison of Magnetic Response of Hole-doped $\text{CuO}_2$ Planes

T. Sasagawa,<sup>1,2</sup> P. K. Mang,<sup>2</sup> O. P. Vajk,<sup>3</sup> A. Kapitulnik,<sup>2,3</sup> and M. G. Reven<sup>2,4</sup>

<sup>1</sup> Department of Advanced Materials Science, University of Tokyo, 7-3-1 Hongo, Bunkyo-ku, Tokyo 113-0033, Japan

<sup>2</sup> Department of Applied Physics, <sup>3</sup>Physics, and <sup>4</sup>Stanford Synchrotron Radiation Laboratory, Stanford University, Stanford, California 94305

May 21, 2019

Although  $\text{La}_2\text{Cu}_{1-x}\text{Li}_x\text{O}_4$  (Li-LCO) differs from  $\text{La}_{2-x}\text{Sr}_x\text{CuO}_4$  (Sr-LCO) in many ways (e.g., absence of metallic transport, high- $T_c$  superconductivity, and incommensurate antiferromagnetic correlations), it has been known that certain magnetic properties are remarkably similar. The present work establishes the detailed bulk magnetic phase diagram of Li-LCO ( $0 < x < 0.07$ ), which is found to be nearly identical to that of lightly-doped Sr-LCO, and therefore extends the universality of the phase diagram to hole-doped but non-superconducting cuprates.

PACS numbers: 74.25.Ha, 74.72.Dn, 75.50.Lk

Depending on the nature and concentration of dopants,  $\text{La}_2\text{CuO}_4$  (LCO) displays a wide variety of phenomena such as antiferromagnetism, spin glass (SG) behavior, anomalous metallic response, and high-temperature superconductivity (HTS). Undoped LCO contains weakly coupled  $\text{CuO}_2$  planes and exhibits antiferromagnetic (AF) order of the  $\text{Cu}^{2+}$  spin-1/2 moments below  $T_N = 325$  K. Replacement of  $\text{Cu}^{2+}$  by non-magnetic  $\text{Zn}^{2+}$  or  $\text{Mg}^{2+}$  models random spin dilution, leading the system into a disordered state at doping concentrations above 40% [1].

On the other hand, substitution of divalent alkaline earth cations for  $\text{La}^{3+}$  or the introduction of excess interstitial oxygen introduces hole charge carriers into the  $\text{CuO}_2$  planes which frustrate the spin system [2]. A concentration of  $x = 0.02$  in  $\text{La}_{2-x}\text{Sr}_x\text{CuO}_4$  (Sr-LCO) is enough to destroy the AF order; this value is one order of magnitude smaller than for the spin-dilution case. Spin freezing has been found at low temperatures in the AF doping regime ( $x < 0.02$ ) [3], with recent direct evidence for electronic phase separation [4]. Further doping ( $x > 0.02$ ) leads to the emergence of a SG phase [5{7}], followed by superconductivity for  $x = 0.06 - 0.25$ . SG order is found to coexist with superconductivity [8], with no apparent anomaly in the SG temperature at the doping level  $x = 0.06$  at which superconductivity first occurs [8{10}]. The phase diagram of the substitutionally-doped bilayer material  $\text{Y}_{1-x}\text{Ca}_x\text{Ba}_2\text{Cu}_3\text{O}_6$  (Ca-YBCO) closely resembles that of Sr-LCO [9], and spin freezing has also been found in both LCO [11] and YBCO [12] doped with excess oxygen.

The extrapolated disappearance of SG order in Sr-LCO and Ca-YBCO appears to coincide with the doping level at which the normal state pseudo-gap extrapolates to zero, and it has been suggested [10,13] that this might be consistent with predictions involving quantum criticality [14]. In the d-density wave picture of HTS [13], the reason for the lack of a genuine phase transition at the pseudo-gap temperature is that the disorder present in all existing cuprates corrupts the d-density wave order and transforms the transition into the low-temperature SG transition. While the freezing

of d-density wave fluctuations is one proposal for the origin of the SG in doped cuprates, there also exist other interpretations [5{7,15{17}]. For example, it has been argued that the glassiness found in doped Mott insulators may be self-generated, due to the competition between interactions on different length scales, and that quenched disorder may merely further stabilize SG order [17]. The most discussed scenario has been the so-called cluster-SG [5,6], with holes on the cluster boundaries and in the clusters giving rise to SG physics and to the experimentally observed incommensurate spin correlations [7].

Given the enormous interest in the connection between magnetic correlations and HTS, it would be valuable to investigate the detailed magnetic properties of related, non-magnetic materials such as  $\text{La}_2\text{Cu}_{1-x}\text{Li}_x\text{O}_4$  (Li-LCO) [18{22]. Since  $\text{Li}^+$  not only provides one hole carrier, but also removes a  $\text{Cu}^{2+}$  spin, this system experiences the dual effects of spin dilution and frustration. Unlike Sr-LCO, Li-LCO does not superconduct [18] and shows no evidence of incommensurate AF correlations [22]. However, early work on polycrystalline samples reported a rapid suppression of AF order with doping [19{21], similar to Sr rather than Zn-doping, and evidence for spin freezing in the Neel state [21]. The remarkable similarity of magnetic properties of lightly doped Li-LCO with those of Sr-LCO has been interpreted as due to new collective behavior of the holes [21]. Therefore, in connection with HTS, the detailed magnetic properties and phase diagram of Li-LCO are of considerable interest. Experimentally, spin-freezing is observed at a different temperature, depending on the time scale of the probe [7,23]. Unlike NQR [3,21], SR [9,10], and neutron scattering [7,4], SQUID magnetometry is essentially a static probe, allowing a more accurate extraction of the SG transition temperature  $T_{sg}$  [6,7]. The present magnetometry study establishes the existence of a nearly quantitative agreement of the bulk magnetic phase diagram of Li-LCO with that of Sr-LCO. Since the strength and type of the disorder as well as the charge transport differ significantly in these two materials, this finding places constraints on the origin of the SG degrees of freedom in

hole-doped cuprates.

Using the traveling-solvent coating-zone method, we have succeeded in growing large single crystals of  $\text{La}_2\text{Cu}_{1-x}\text{Li}_x\text{O}_4$  ( $0 < x < 0.07$ ). In order to eliminate possible hole doping by excess oxygen, the crystals were carefully heat treated under reducing conditions. The Li concentrations were estimated to within 0.003 from x-ray diffraction measurements of the lattice constants [20]. For a few samples, we confirmed this estimate using neutron diffraction to determine structural and Néel transition temperatures [20]. All magnetometry data reported here were taken with the magnetic field along the tetragonal  $a$ -axis.

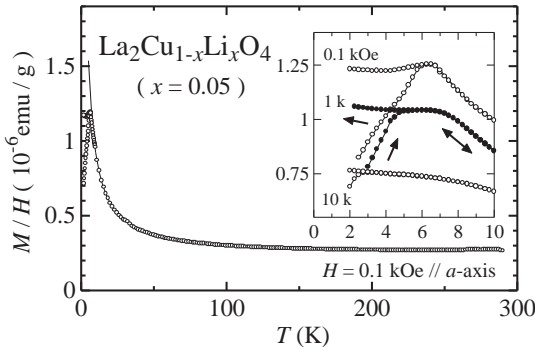


FIG. 1. Magnetic susceptibility of  $\text{La}_2\text{Cu}_{0.95}\text{Li}_{0.05}\text{O}_4$ . A magnetic field  $H = 0.1$  kOe was applied parallel to the tetragonal  $a$ -axis. The solid curve is a Curie-Weiss fit of the high-T data. The inset shows the low-T behavior at various fields. Arrows indicate the T-scan directions.

For  $x < 0.03$ , the doping dependences of the Néel temperature determined by both local [19,21] and bulk [20] magnetic probes agree quite well, and therefore the AF phase boundary has been well determined as in Sr-LCO. SR study indicates magnetic order at low temperatures even up to  $x = 0.10$  [19], but bulk magnetization measurements only show spin paramagnetism for  $x > 0.03$  [20]. The temperature dependent susceptibility for  $x > 0.03$  can therefore be expressed by the extended Curie-Weiss formula:

$$\langle T \rangle = \langle_0 + C = \langle T - T_c \rangle; \quad (1)$$

where  $\langle_0$ ,  $C$ , and  $T_c$  are the T-independent susceptibility, Curie constant, and Curie-Weiss temperature, respectively. Figure 1 shows  $\langle T \rangle$  for  $x = 0.05$ . As in the earlier powder report [20], paramagnetism is observed in the high-T regime. A fit to Eq. (1) [solid line in Fig. 1] resulted in  $\langle_0 = 2.35 \times 10^{-7}$  emu/g,  $C = 7.18 \times 10^{-6}$  emu K/g, and  $T_c < 0.5$  K. We note that these parameters are roughly comparable with those Sr-LCO:  $\langle_0 = 0.4 \times 10^{-7}$  emu/g for  $x = 0.04$  [6],  $C = 2.5 \times 10^{-6}$  emu K/g, and  $T_c = 0$  K for  $x = 0.03$  [6,7].

At low temperatures,  $\langle T \rangle$  deviates significantly from a Curie-Weiss law and shows signatures of a SG. As thoroughly described later by the appropriate limits of the scaling function, the SG order parameter in the zero-

eld limit increases from zero upon cooling below  $T_{sg}$ , which decreases ( $T$ ) for  $T < T_{sg}$ . Besides, the resulting peak becomes broader as the applied magnetic field is increased [inset of Fig. 1] due to the enhancement of the order parameter both above and below  $T_{sg}$ . From the peak in the lowest field ( $H = 0.1$  kOe) we determined  $T_{sg} = 6.2(1)$  K, which should be compared to  $T_{sg} = 5.0(5)$  K for Sr-LCO with  $x = 0.05$  [7]. Hysteresis below  $T_{sg}$ , observed between zero-field-cooled and field-cooled curves, is indicated with the help of arrows in the inset of Fig. 1. Such behavior is also characteristic of a SG. Observing these features in either small crystals or polycrystalline samples would be difficult because they become obscured as the field is increased, or when the field direction is canted away from the  $\text{CuO}_2$  plane.

We have further characterized the SG state by means of a scaling analysis of the SG order parameter  $q$ , which is associated with the deviation of the observed equilibrium (field-cooled) susceptibility ( $T; H$ ) from Curie behavior [24]. Normalization to satisfy  $0 \leq q \leq 1$  yields

$$q(T; H) = [(\langle_0 + C = T) - \langle T; H \rangle] / (C = T); \quad (2)$$

Using the reduced temperature  $t = (T - T_{sg})/T_{sg}$  and a scaling function  $F(z)$ , the SG order parameter is

$$q(T; H) = \frac{t}{\beta} F(H^2/t^{\phi}); \quad (3)$$

where  $\beta$  and  $\phi$  are the critical exponents characterizing the SG state [24].  $F(z)$  is well known in the following three limits: (i)  $F_+(z \neq 0) = 0$  ( $t > 0$ ), (ii)  $F_-(z \neq 0) = \text{const.}$  ( $t < 0$ ), and (iii)  $F_0(z \neq 1) = z^{-\phi}$ . As shown in Fig. 2(a) for  $x = 0.05$ , (ii) gives the estimate  $\beta = 0.7(1)$ . Similarly, using (iii),  $\phi$  can be determined from  $q(T_{sg}; H) = (H^2)^{\phi} = 1$ . The slope in Fig. 2(b) then gives  $\phi = 0.163(5)$ .

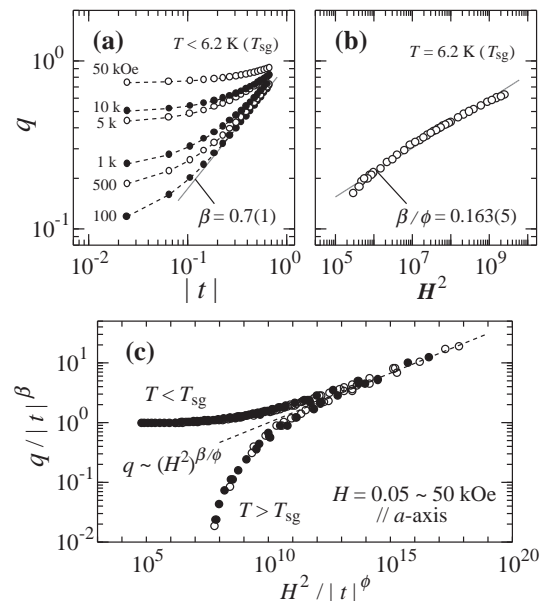


FIG. 2. Scaling analysis of the data in Fig. 1. SG order parameter  $q$  as a function of (a) reduced temperature  $t$  and (b) field squared  $H^2$ . (c) Scaling plot of the SG order parameter.

Through the process of getting the best scaling result, shown in Fig. 2(c), the critical exponents have been optimized further:  $\alpha = 0.78(5)$  and  $\beta = 4.1(5)$ . The same SG features were observed for  $x = 0.06$  and  $0.07$ . The critical exponents obtained in this manner do not depend on  $x$ , although  $T_{sg}$  decreases with  $x$ . We note that, in addition to the comparable values of  $T_{sg}$ , the critical exponents are found to be almost identical to those of Sr-LCO [6,7], suggesting the existence of the same SG state in both systems. While the observed exponents are consistent with those of canonical SG materials [6], recent results for untwinned Sr-LCO crystals reveal unconventional anisotropic behavior [25].

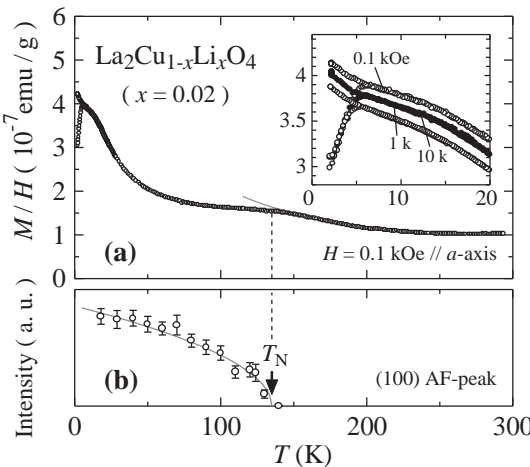


FIG. 3. (a)  $M/H(T)$  of  $\text{La}_2\text{Cu}_{0.98}\text{Li}_{0.02}\text{O}_4$  as a function of temperature under  $H = 0.1$  kOe. The inset magnifies the low-T behavior at various fields. (b)  $T$ -dependence of the integrated intensity of the (100) antiferromagnetic neutron peak (orthorhombic notation). The  $t$  (solid curve) gives  $T_N = 135$  K, which corresponds well to the peak in the susceptibility.

For  $x < 0.03$ , the magnetic susceptibility differs from that for  $x > 0.03$ . Data for  $x = 0.02$  are shown in Fig. 3(a). Two magnetic anomalies are present. One is a high-T cusp associated with the AF transition [20]. As shown in Fig. 3(b), neutron data complement the SQUID observations, providing unambiguous evidence of a well-defined Néel transition at  $T_N = 135$  K. The second anomaly appears somewhat analogous to the SG behavior found for  $x > 0.03$  in that we find hysteresis below the anomaly and the onset temperature of magnetic irreversibility is comparable to  $T_{sg}$  for  $x > 0.03$ . Local-probe  $^{139}\text{La}$ -NQR and SR experiments indicate a corresponding spin-freezing within the AF state in Sr-LCO [3,9] and Li-LCO [21]. This has been ascribed to the continuous freezing of the spins of the doped holes on the antiferromagnetic background [3], with independent ordering of  $\text{Cu}^{2+}$  spins and doped holes [9], or due to new collective hole behavior [21]. However, to the best of our knowledge, this spin freezing has not been reported thus far from bulk magnetometry for the cuprates. Although the second anomaly appears to be a SG transition, further

characterization in terms of critical scaling analysis is not possible due to the ambiguity in the definition of the SG order parameter. We define the characteristic freezing temperature,  $T_f$ , as the lower-T "shoulder" of the zero-field-cooled data at low  $H$ , which corresponds to the onset of magnetic hysteresis for  $x = 0.02$ , as seen in the inset of Fig. 3(a). We note that, although not shown here, a change in the imaginary part of the AC susceptibility was also observed at this temperature, which can be associated with the drastic change of the spin response due to the onset of the spin-freezing.

Our results yield the phase diagram summarized in Figure 4. NQR ( $x < 0.02$ ) [3] and magnetometry ( $x > 0.02$ ) [7] data from Sr-LCO single crystals are included for comparison. Despite the different nature of the dopants, the phase boundaries for these two compounds are almost identical. Fig. 4 demonstrates that  $T_f \propto x$  as in Sr-LCO, opposite to the trend with doping for either  $T_N$  or  $T_{sg}$ . We find  $T_f = (339(14)$  K)  $\propto x$ , as compared to  $T_f = (815$  K)  $\propto x$  for Sr-LCO from  $^{139}\text{La}$  NQR [3].

The dopant concentrations at which Néel order is lost in the two materials differ by a factor of 2/3. Qualitatively, this shift of the phase boundaries can be understood to result from reduced magnetic frustration in the Li-doped system [27]. As shown in the inset of Fig. 4, when scaled by that factor,  $T_{sg}$  for Li-LCO ( $x > 0.03$ ) quantitatively agrees with the SG temperature for Sr-LCO. Since NQR and magnetometry probe very different time scales, systematic Sr-LCO magnetometry data for  $x < 0.02$  would be very desirable for a proper quantitative comparison at low doping.

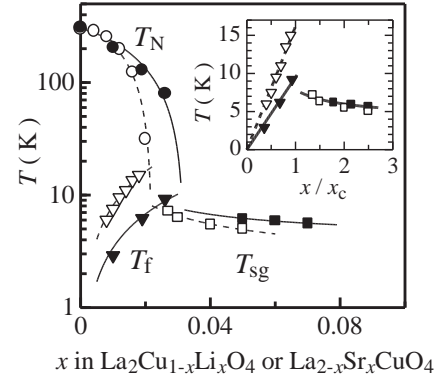


FIG. 4. Magnetic phase diagram for  $\text{La}_2\text{Cu}_{1-x}\text{Li}_x\text{O}_4$  (filled symbols) and  $\text{La}_{2-x}\text{Sr}_x\text{CuO}_4$  (open symbols; from NQR ( $x < 0.02$ ) [3] and magnetometry ( $x > 0.02$ ) [7]): circles for the Néel temperature  $T_N$ , triangles for the onset of the SG-like anomaly  $T_f$ , and squares for the SG temperature  $T_{sg}$ . Inset: scaled phase diagram.

Recent neutron scattering results reveal direct evidence for electronic phase separation in Sr-LCO ( $x < 0.02$ ) into regions with hole concentrations  $\sim 0$  and  $\sim 0.02$  [4]. The latter phase exhibits diagonal stripes [7]. Spin freezing occurs below the doping-independent phase separation temperature  $T_{ps} \sim 30$  K determined from neu-

tron scattering [4], and consistent with previous NQR results [3]. For Li-LCO, on the other hand, commensurate AF correlations have been both predicted [28] and observed [22], consistent with the expected stronger pinning potential of the in-plane dopant  $\text{Li}^+$ . Consequently, the cluster model of Ref. [16], originally proposed for Sr-LCO, but which predicts commensurate AF correlations, might more accurately describe the physics of the Li-doped variant. This model predicts  $k_B T_f \propto J_e x$ , where  $J_e$  is the effective in-plane exchange coupling constant [16]. While this linear doping dependence is indeed consistent with our observations, the same behavior is found in Sr-LCO [3]. On the other hand, it has been speculated that  $T_f$  in Sr-LCO might depend linearly on the volume fraction of the SG phase [4]. The close analogy between the NQR [3,21] and bulk magnetic properties of the two materials suggests that Li-LCO might phase separate as well.

At higher hole concentrations, the behavior of the carriers differs significantly between Li-LCO and Sr-LCO. The latter material shows an insulator to metal transition and HTS, while the former remains insulating. What is particularly interesting from our present observations is that, in spite of the great difference in charge dynamics for  $x > 0.03$ , the spin degrees of freedom measured via magnetometry are remarkably similar in both compounds. We note that the unscaled values of  $T_{\text{sg}}(x)$  for the more disordered material Li-LCO lie above those of Sr-LCO, contrary to suggestions that increased disorder should suppress  $T_{\text{sg}}(x)$  [13]. The relative shift of the SG phase boundaries likely results from an effective decrease of magnetic frustration due to the presence of non-magnetic  $\text{Li}^+$  in Li-LCO [27]. The insensitivity of the low-temperature phase boundaries to the type and strength of the quenched disorder is consistent with the notion that the glassiness in these doped Mott insulators is primarily self-generated [17].

In summary, the bulk magnetic properties of Li-LCO single crystals are found to be richer than previously reported from powder samples. Our results demonstrate the feasibility of extracting low-temperature freezing temperatures in the Néel state from magnetometry, and call for similar measurements in other cuprates for a proper quantitative comparison. We find that  $T_f \propto x$ , which has previously been reported for Sr-LCO as well. Since the spin freezing in the latter material occurs in a phase separated state, the close similarity between the doping dependence of the freezing temperature suggests that lightly-doped Li-LCO might phase separate as well, despite the stronger pinning potential of the in-plane dopant  $\text{Li}^+$ . Outside of the Néel phase, the spin glass phase boundaries differ by a mere scale factor for the effective doping level. The experimental results for Li-LCO obtained here extend the universality of the phase diagram to hole-doped but non-superconducting cuprates.

We thank D. Fisher, H. Eisaki, K. Kishio, R.S. Markiewicz, Ch. Niedermayer, C. Panagopoulos, and H. Takagi for fruitful discussions. P.K.M. and M.G. would

like to thank the staff of the NIST Center for Neutron Research for their warm hospitality. The work at Stanford was supported by the U.S. DOE under Contract Nos. DE-FG 03-99ER 45773 and DE-AC 03-76SF 00515, by NSF CAREER Award No. DMR 9400372, and by the A.P. Sloan Foundation. T.S. was partially supported by JSPS.

---

- [1] O.P. Vajk et al., *Science* 295, 1691 (2002).
- [2] A. Aharony et al., *Phys. Rev. Lett.* 60, 1330 (1988).
- [3] F.C. Chou et al., *Phys. Rev. Lett.* 71, 2323 (1993), F. Borsig et al., *Phys. Rev. B* 52, 7334 (1995).
- [4] M.M. Atsuda et al., *Phys. Rev. B* 65, 134515 (2002).
- [5] J.H. Cho et al., *Phys. Rev. B* 46, 3179 (1992).
- [6] F.C. Chou et al., *Phys. Rev. Lett.* 75, 2204 (1995).
- [7] S. Wakimoto et al., *Phys. Rev. B* 62, 3547 (2000).
- [8] H. Kitazawa, K. Katsumata, E. Torikai, and K. Nagami, *Solid. State. Commun.* 67, 1191 (1988); A. Weidinger et al., *Phys. Rev. Lett.* 62, 102 (1989).
- [9] Ch. Niedermayer et al., *Phys. Rev. Lett.* 80, 3843 (1998).
- [10] C. Panagopoulos, B.D. Rainford, J.R. Cooper, and C.A. Scott, *Physica (Amsterdam)* 341C, 843 (2000); C. Panagopoulos et al., cond-mat/0007158.
- [11] V.Yu. Pomjakushin et al., *Physica (Amsterdam)* 272C, 250 (1996).
- [12] R.F. Kie et al., *Phys. Rev. Lett.* 63, 2136 (1989).
- [13] S. Chakravarty, R.B. Laughlin, D.K. Morr, and C. Nayak, *Phys. Rev. B* 63, 094503 (2001).
- [14] S. Andergassen, S. Caprara, C. Di Castro, and M. Grilli, *Phys. Rev. Lett.* 87, 056401 (2001), and references therein.
- [15] V.J. Emery and S.A. Kivelson, *Physica (Amsterdam)* 209C, 597 (1993); S.A. Kivelson and V.J. Emery, cond-mat/9809082.
- [16] R.J. Gooding, N.M. Salem, R.J. Birgeneau, and F.C. Chou, *Phys. Rev. B* 55, 6360 (1997).
- [17] J. Schmalian and P.G. Wolyne, *Phys. Rev. Lett.* 85, 836 (2000); H. Westfahl, Jr., J. Schmalian, and P.G. Wolyne, *Phys. Rev. B* 64, 174203 (2001).
- [18] M.A. Kastner et al., *Phys. Rev. B* 37, 111 (1988).
- [19] L.P. Le et al., *Phys. Rev. B* 54, 9538 (1996).
- [20] J.L. Sarrao et al., *Phys. Rev. B* 54, 12014 (1996).
- [21] B.J. Suh et al., *Phys. Rev. Lett.* 81, 2791 (1998).
- [22] W. Bao et al., *Phys. Rev. Lett.* 84, 3978 (2000); W. Bao and J.L. Sarrao, cond-mat/0203318.
- [23] R.S. Markiewicz, F.C. Odero, A.P. Paolone, and R.C. Cantelli, *Phys. Rev. B* 64, 054409 (2001), and references therein.
- [24] A.P. Malozemoff, S.E. Barnes, and B. Barbara, *Phys. Rev. Lett.* 51, 1704 (1983); B. Barbara, A.P. Malozemoff, and Y. Imry, *ibid.* 47, 1852 (1981).
- [25] A.N. Lavrov, Y. Ando, S. Komiyama, and I.T. Suzuki, *Phys. Rev. Lett.* 87, 017007 (2001).
- [26] J.H. Cho, F.C. Chou, and D.C. Johnston, *Phys. Rev. Lett.* 70, 222 (1993).
- [27] I.Ya. Korenblit, A. Aharony, and O. Entin-Wohlman, *Phys. Rev. B* 60, 15017 (1999).
- [28] C. Buhler, S. Yunoki, and A.M. Oero, *Phys. Rev. B* 62, 3620 (2000).